

# Design and characterization of TES bolometers and SQUID readout electronics for a balloon-borne application

Johannes Hubmayr<sup>a</sup>, François Aubin<sup>b</sup>, Eric Bissonnette<sup>b</sup>, Matt Dobbs<sup>b</sup>, Shaul Hanany<sup>a</sup>,  
Adrian T. Lee<sup>c</sup>, Kevin MacDermid<sup>b</sup>, Xiaofan Meng<sup>c</sup>, Ilan Sagiv<sup>a</sup>, Graeme Smecher<sup>b</sup>

<sup>a</sup>University of Minnesota School of Physics and Astronomy, Minneapolis, MN 55455;

<sup>b</sup>McGill University, Montréal, Quebec, H3A 2T8, Canada;

<sup>c</sup>University of California, Berkeley, Berkeley, CA 94720

## ABSTRACT

We present measurements of the electrical and thermal properties of new arrays of bolometric detectors that were fabricated as part of a program to develop bolometers optimized for the low photon background of the EBEX balloon-borne experiment. An array consists of 140 spider-web transition edge sensor bolometers microfabricated on a 4" diameter silicon wafer. The designed average thermal conductance ( $\bar{G}$ ) of bolometers on a proto-type array is 32 pW/K, and measurements are in good agreement with this value. The measurements are taken with newly developed, digital frequency domain multiplexer SQUID readout electronics.

**Keywords:** Bolometer, Transition edge sensor, CMB, SQUID, Balloon-borne

## 1. INTRODUCTION

Improvements in millimeter-wavelength instrument sensitivity are now achievable through the development of large format bolometer arrays cooled to sub-Kelvin temperatures. Single bolometers have been demonstrated to yield sensitivity close to the limit set by photon noise. Thus, increased sensitivity can only be achieved with large numbers of detectors. Superconducting transition edge sensor (TES) bolometers are a suitable choice to make arrays because they can be fabricated using standard thin film deposition and optical lithography techniques.<sup>1</sup> The TES bolometer also has the advantage of strong negative electro-thermal feedback which increases the linearity, dynamic range and speed of the device.<sup>2</sup> Readout electronics based on multiplexing superconducting quantum interference devices (SQUIDs) are now capable of reading out large arrays of TES bolometers. Multiplexing is a key technology which decreases the heat load on the sub-Kelvin detector stage as well as the cost and complexity of cold wiring. Time domain multiplexing has been developed by NIST<sup>3</sup> and an analog frequency domain multiplexer (fMUX) system has been developed by a collaboration between University of California, Berkeley (UCB) and Lawrence Berkeley National Laboratory (LNBL).<sup>4</sup>

Several ground-based experiments are now fielding these technologies including APEX-SZ,<sup>5</sup> the South Pole Telescope (SPT)<sup>6</sup> and the Atacama Cosmology Telescope (ACT)<sup>7</sup> to probe the Cosmic Microwave Background (CMB) radiation. Observation at frequencies above 250 GHz are difficult from the ground and can provide critical information for CMB experiments such as characterizing the dust foreground. We are building a balloon-borne experiment called EBEX<sup>8</sup> that is designed to measure the polarization of the CMB and will implement 1440 TES bolometers with SQUID based multiplexed readouts. EBEX will have three frequency bands centered around 150, 250 and 410 GHz, each with  $\sim 30\%$  bandwidth.

The lower atmospheric loading and colder telescope temperature at balloon altitudes allow substantial sensitivity gains by lowering the thermal conductance of the bolometer. The designed average thermal conductance ( $\bar{G}$ ) of the EBEX 150 GHz bolometers is 10 pW/K. The designed optical time constant is 3 ms.

---

Contact Author: J.Hubmayr

Email: hubmayr@physics.umn.edu

Telephone: 612.626.9149

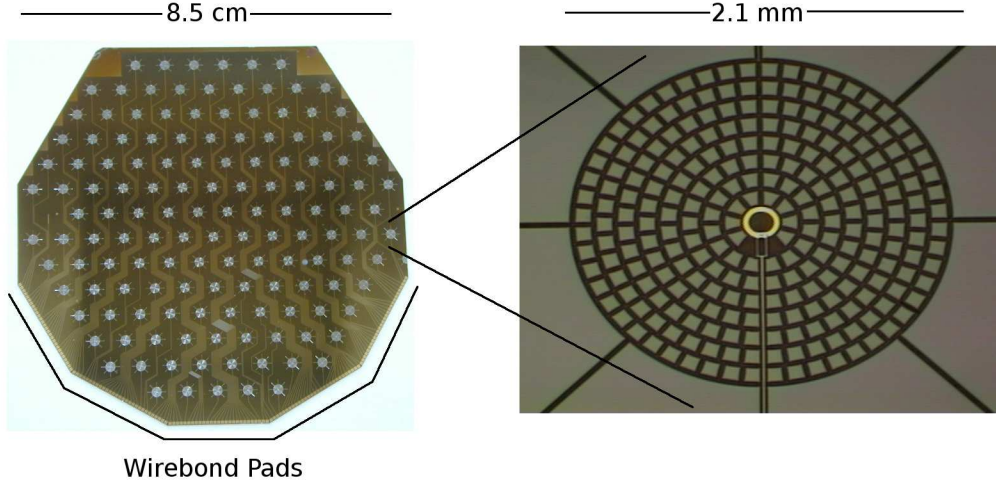


Figure 1. **Left:** The 140 element transition edge sensor (TES) bolometer array. **Right:** A close up picture of a spider-web TES bolometer. The gold ring and TES can be seen in the middle of the picture with the superconducting leads exiting the bottom of the picture.

In this paper we report measurements of a prototype array of bolometers that was fabricated as a step in achieving the low thermal conductance necessary for EBEX. This array was designed to have  $\bar{G} = 32$  pW/K and a predicted time constant of 3 ms.

The measurements were performed with digital frequency domain multiplexer (DfMUX) electronics developed at McGill University.<sup>9</sup> The DfMUX system is an upgrade from the analog fMUX system and was specifically designed for the low power consumption requirements of a balloon experiment.

## 2. BOLOMETER ARRAY

The left panel of Fig. 1 shows a photograph of the prototype bolometer array, which was fabricated in the Berkeley Microlab clean-room facility using standard thin film deposition and optical lithography. The array contains 140 spider-web TES bolometers spaced 6.6 mm apart center-to-center. Superconducting aluminum leads connect each TES to wirebonding pads at the bottom five sides of the wafer. One of the bolometers is shown in the right panel of Fig. 1. The bolometer consists of three main structures: a spider-web absorber, a TES and a gold ring. The 2.1 mm diameter spider-web absorber is composed of 1  $\mu\text{m}$  thick, 6  $\mu\text{m}$  wide low-stress silicon nitride and has a 117  $\mu\text{m}$  grid spacing. The spider web geometry is chosen to reduce heat capacity as well as the cross-section to cosmic rays. The web is metallized with a 2  $\mu\text{m}$  wide, 12 nm thick layer of Au which has a DC sheet resistance  $\sim 200$   $\Omega$  per square. The spider web is thermally isolated from the heatsink by silicon nitride legs that have a ratio of cross-sectional area to length  $A/l = 132$  nm. The transition edge sensor is composed of an Al/Ti proximity effect sandwich tuned to have a  $\sim 1$   $\Omega$  normal resistance and transition temperature  $T_c \sim 500$  mK. The sensor is thermally attached to a gold ring. The heat capacity of the gold ring limits the sensor bandwidth ensuring stability.<sup>10</sup> The backside of the 500  $\mu\text{m}$  thick wafer is coated with a 250 nm layer of gold creating a  $1/4\lambda$  backshort at 150 GHz, near the peak of the CMB spectrum.

We predict the dynamic thermal conductance of the bolometers using  $G = 4\sigma AT^3\xi$ ,<sup>11</sup> where  $\sigma=15.7\text{mW}/\text{cm}^2\text{K}^4$  and  $T$  is the temperature of the TES. We use the complete diffuse surface scattering limit known as the Casimir limit  $\xi \approx \sqrt{A}/l$  which is valid for  $\sqrt{A}/l \ll 1$ . We predict  $G = 61$  pW/K at  $T_c$ . The relationship between the average thermal conductance ( $\bar{G}$ ) and the dynamic thermal conductance ( $G$ ) is<sup>12</sup>

$$G/\bar{G} = \frac{(n+1)(1-T_s/T_c)}{1-(T_s/T_c)^{n+1}} \quad (1)$$

assuming the thermal conductivity follows  $\kappa \sim T^n$ . Heat conduction from the bolometer to heatsink is dominated by silicon nitride, which has an index  $n = 3$ . Using Eqn. 1 we predict  $\bar{G} = 32$  pW/K.

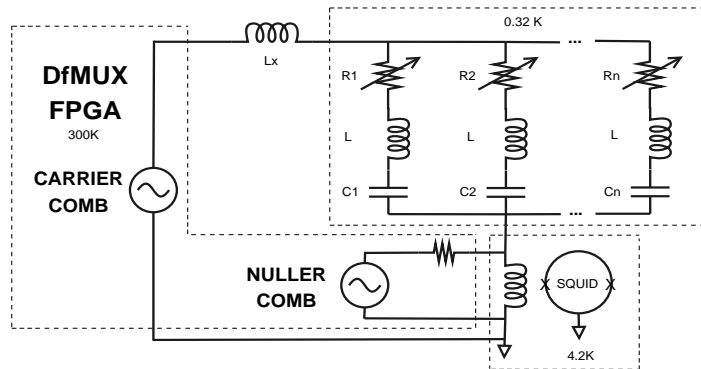


Figure 2. Electrical schematic of the readout system. The multiplexed module is held at 320 mK. The bolometers in the module are voltage biased with a comb of sine wave carriers. Currents from the bolometers are read out with a SQUID ammeter at 4.2 K. The carrier amplitudes are removed with a nuller comb. The carrier and nuller combs are produced with an FPGA on the DfMUX readout boards described in Sec. 3.2.  $L_x$  is the stray inductance in series with the module discussed in Sec. 5.1.

### 3. READOUT

#### 3.1 Principle

We use SQUID based frequency domain multiplexing to readout the bolometer arrays. An electrical schematic of the readout system is shown in Fig. 2. The  $\sim 1 \Omega$  transition edge sensors of the bolometer array are placed in series with band defining LC filters. The LCR circuits are wired in parallel to create a multiplexed module. A comb of sine wave carriers between 300 kHz - 1 MHz voltage biases each sensor in the module at its LC resonant frequency. Sky intensity changes the sensor resistance and amplitude modulates the carrier transferring signals to the side-bands of each carrier. Thus each sensor response is well defined in frequency space. Currents from all sensors within the module are carried on a single pair of wires to a SQUID ammeter. Warm electronics are used to lock in on the carrier frequency of each sensor with a bandwidth that contains the sky signal.

The large carrier amplitudes of the module present a flux burden on the SQUID. Since there is no sky signal at the carrier frequencies, they can be removed. A nuller comb consisting of sine wave currents 180 degrees out of phase with each carrier frequency is summed at the SQUID input. This nuller comb removes the unmodulated carrier amplitudes reducing the dynamic range requirement of the SQUID and increasing linearity.

#### 3.2 DfMUX

We use new digital frequency domain multiplexer (DfMUX) electronics for our implementation of frequency domain multiplexing. The DfMUX boards are a drop-in replacement for the analog fMUX boards designed to consume substantially less power and improve low frequency noise performance.<sup>9</sup> The DfMUX board shown in Fig. 3 produces the sine wave carrier and nuller combs digitally with a Xilinx Virtex4 LX160 FPGA. The SQUID output is directly digitized with an ADC operating at 25 MHz. Sky signal from each bolometer is then digitally demodulated with a set of parallel algorithms that use a half-wave mixer and a series of cascading filters. As such the mixer is sensitive to odd harmonics of the fundamental frequency with a response that falls off as  $1/(2n + 1)$ , where  $n$  is an integer.

Placing sine wave generation and signal demodulation in the digital domain achieves substantial power savings over the previous implementation of the frequency multiplexing system, which performed these functions in the analog domain. The power consumption of one DfMUX board is 16 W and is capable of reading out four modules with multiplexing factors of 32. The DfMUX system is therefore capable of dissipating as little as 125 mW per detector. However, the multiplexer bandwidth is currently limited by the cold components of the system. Using a multiplexing factor of 12 to readout 1440 detectors, as is planned for EBEX, the power consumption of the readout system is 565 W, which includes a 15% loss of efficiency in power delivery. This level of power consumption satisfies the EBEX power budget constraints.

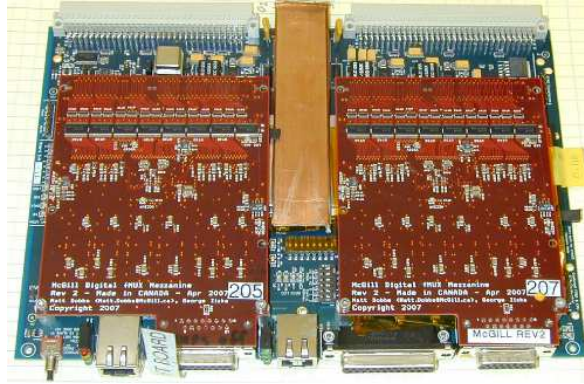


Figure 3. The digital frequency domain multiplexer (DfMUX) readout board developed at McGill University is shown. Two mezzanine boards which house the majority of the analog components attach to the FPGA motherboard. One board can readout 128 bolometers and dissipates 16W.

The DfMUX boards contain a set of algorithms to tune and monitor the SQUIDs and detectors. This functionality is essential for commanding the readout system remotely during a balloon flight. The measurements described in Sec. 5 are taken with automated scripts run by the DfMUX boards.

## 4. EXPERIMENTAL SETUP

The prototype bolometer array is heatsunk to the baseplate of a  $^3\text{He}$  adsorption refrigerator<sup>13</sup> operated at 320 mK. The array is enclosed in a dark cavity at the same temperature so that radiative loading is negligible. A Fairchild LED56 inside the dark cavity provides optical signals to the bolometers. Each bolometer is wired in series with a ceramic capacitor<sup>14</sup> and a  $16 \mu\text{H}$  inductor fabricated by TRW. Using a multiplexing factor of three, the bolometers are read out with a 100 series array SQUID amplifier<sup>15</sup> operated in shunt feedback coupled to a room temperature amplifier located on a custom SQUID Controller electronics board.<sup>16</sup> The SQUID is heatsunk to 4.2 K. The output of the SQUID is sent on a twisted pair to the demodulator of the DfMUX board.

## 5. RESULTS

### 5.1 Network Analysis

In order to determine the bias frequencies, normal resistance of the bolometers and the stray inductance in series with the module, we perform the network analysis shown in Fig. 4. For this measurement, the cold stage is held above the TES transition at 800 mK, and a carrier voltage sweeps across the module in frequency. The three peaks at 438, 534 and 645 kHz are the LC resonant frequencies in series with sensors ‘11-01’, ‘10-02’ and ‘9-03’ respectively. We fit the data to an analytic circuit model with  $2n + 1$  free parameters where  $n$  is the number of bolometer channels. The inductors in series with each bolometer are fixed at  $16 \mu\text{H}$ , and the voltage bias is fixed at  $3.9 \mu\text{V}_{\text{rms}}$ . For each channel the normal resistance of the bolometer and the capacitance in series with the bolometer are to be determined from the fit. The stray inductance in series with the module ( $L_x$ , as shown in Fig. 2) is also determined by the fit. The impedance of the stray inductance ( $\omega L_x$ ) creates a frequency dependant voltage divider which is the source of the decreasing peak height with increasing frequency. Since the voltage bias of the bolometer ( $V_b$ ) largely determines the responsivity of the device,<sup>12</sup> it is important to determine  $L_x$ . From the fit, we determine that  $R = 1.03, 1.04$  and  $1.00 \Omega$  for bolometers ‘11-01’, ‘10-02’ and ‘9-03’ respectively, and  $L_x = 149 \text{ nH}$ . For all TES,  $L_x$  affects the voltage bias by  $< 10\%$ . However, for subsequent measurements, we include  $L_x = 149 \text{ nH}$  in our analysis.

### 5.2 Thermal Conductance

To determine the average thermal conductance of the bolometers ( $\bar{G}$ ), we perform current versus voltage (IV) measurements of the three bolometers in the module. Each sensor is biased at its resonant frequency, the voltage

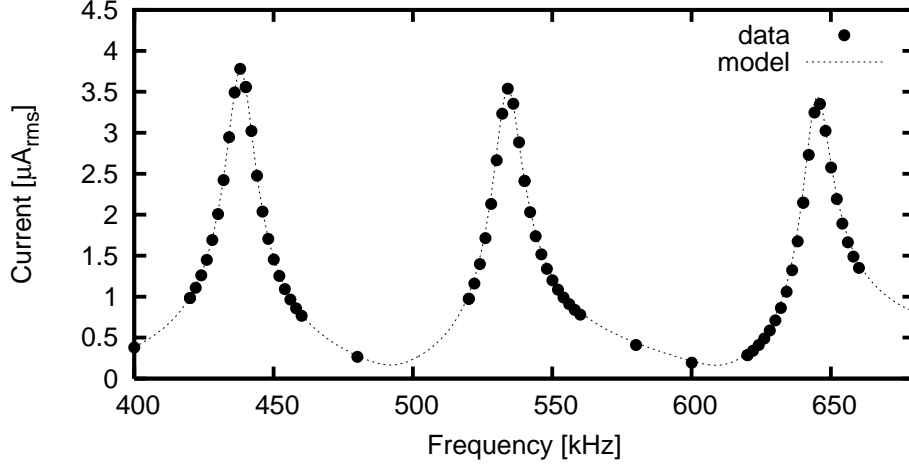


Figure 4. The network analysis of the multiplexed module. A fit to the analytic model shown by the dashed curve is used to determine the bias frequencies, resistance of the bolometers and the stray inductance in series with the module.

is stepped down and the current through the SQUID is recorded. At voltage biases  $> 3\mu V_{rms}$  shown in Fig. 5, the TES is normal and the IV curve is linear. The turnaround at  $\sim 2.5\mu V_{rms}$  is evidence that the TES enters the superconducting transition. In the transition, the total power is constant due to strong electro-thermal feedback, and the current is proportional to the inverse of the voltage bias.

$$P_{rad} + P_{elect} = \bar{G}(T_{tes} - T_s), \quad (2)$$

where  $P_{rad}$  is the radiative power,  $P_{elect} = V_b^2/R_{tes}$  is the electrical power,  $\bar{G}$  is the average thermal conductance,  $T_{tes}$  is the temperature of the TES and  $T_s$  is the temperature of the heatsink. Since the bolometers are operated within a dark enclosure, the data in Fig. 5 together with  $T_c - T_s$  yield measurements of  $\bar{G}$ . We determine  $T_c \sim 550$  mK by biasing the bolometers with  $\sim 10$  nV<sub>rms</sub> and monitoring the current response while slowly lowering the heatsink temperature. We measure  $\sim 32$ , 27 and 33 pW/K for bolometers ‘11-01’, ‘10-02’ and ‘9-03’ respectively, which are in good agreement with the theoretically calculated  $\bar{G} = 32$  pW/K.

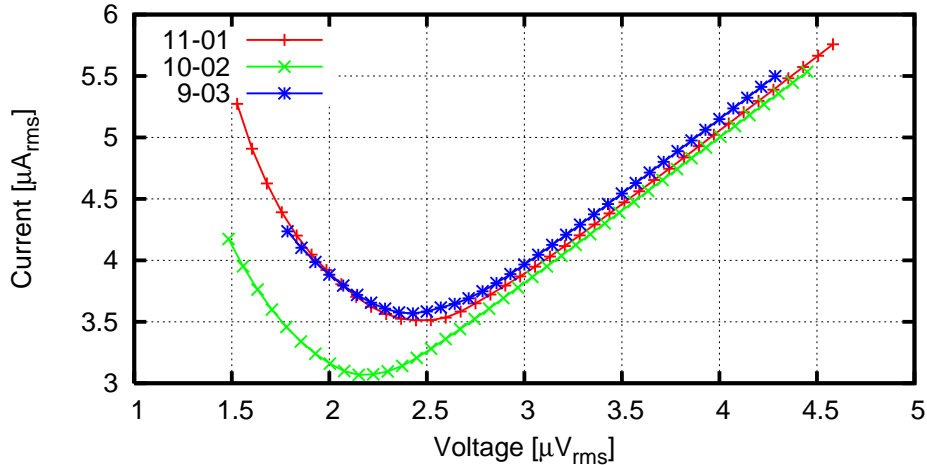


Figure 5. Current versus voltage curves for the bolometers in the module. The electrical power at the turnaround divided by  $T_c - T_s$  gives  $\bar{G} = 32$ , 27 and 33 pW/K for the three devices.

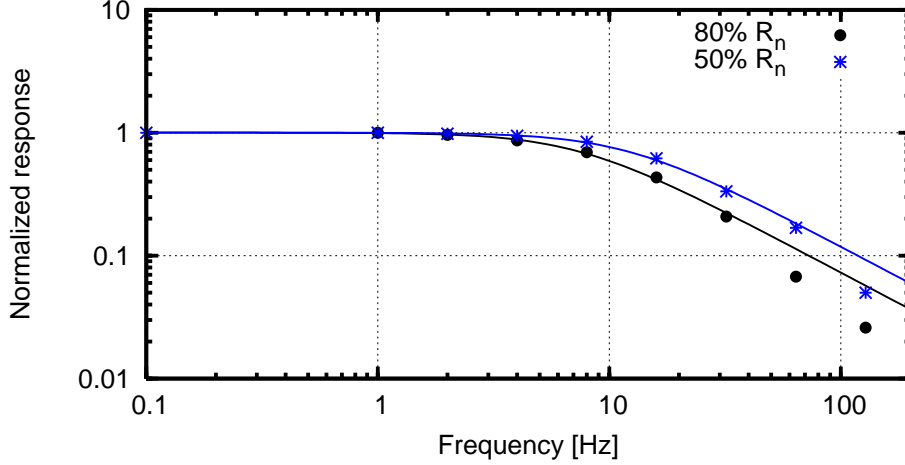


Figure 6. The optical frequency response of bolometer ‘9-03’ biased to  $0.8 \Omega$  (black dots) and  $0.5 \Omega$  (blue asterisks). The single pole fits yield 22 ms and 13 ms time constants.

### 5.3 Optical frequency response

We determine the bolometer response to optical signals by biasing the LED with a small sinusoidal current and measuring the bolometer amplitude response as a function of LED bias frequency. Figure 6 shows the frequency response of bolometer ‘9-03’ biased at  $0.8 \Omega$  (black circles) and  $0.5 \Omega$  (blue asterisks). A single-pole fit gives optical time constants of 22 ms and 13 ms respectively. With feedhorns coupled to the bolometers we expect the response time to decrease by a factor of  $\sim 2$ -3, which yields a response time close to our design goals when biased at  $0.5 \Omega$ .

The decreased time constant lower into the transition is evidence that the thermalization of the TES, not the spider-web, dominates the response time of the bolometer. For bolometer arrays currently in fabrication we have reduced the heat capacity of the gold ring by a factor of four, which should decrease the response time of the TES by the same factor. The optical response time of the bolometer should then be limited by the thermalization time of the web.

### 5.4 Bolometer Noise

The demodulated noise spectrum of bolometer ‘9-03’ is shown in Fig. 7. The solid, red curve shows the noise level of the bolometer when it is biased with  $2.275 \mu V_{rms}$  and has a resistance of  $0.8 \Omega$ . The spectrum is white down to 200 mHz with an amplitude of  $5.0 \times 10^{-17} W/\sqrt{Hz}$ . The blue, dot-dashed spectrum shows the noise of the bolometer when biased above the transition at  $1.0 \Omega$  and is therefore insensitive to phonon noise. For this bias position the expected noise sources are bolometer Johnson, SQUID and readout electronics noise. The readout noise level is shown in the green, dashed curve. Readout noise consists of SQUID noise and readout electronics noise. When biased to  $0.8 \Omega$  the expected noise level is  $4.2 \times 10^{-17} W/\sqrt{Hz}$ , which is calculated from the quadrature sum of readout, bolometer Johnson and phonon noise using the measured thermal conductance value. The 20% discrepancy between the calculated and measured noise levels is currently under investigation.

The expected noise sources and levels for bolometer ‘9-03’ are listed in Tab. 1 in NEP units. The demodulator transfer function is different for signal and the different noise components of the system. To account for these differences a factor of  $\pi/2$  has been included for the SQUID and readout electronics noise levels, and a factor of  $\sqrt{2}$  has been included for the bolometer Johnson noise.

Post-demodulation the readout noise is increased by a factor 1.5 due to the half-wave mixer’s sensitivity to odd harmonics of the demodulator frequency. A measurement of the pre-demodulated noise level shows an increase in noise at frequencies between 1 and 10 MHz. Since the mixer is sensitive to odd harmonics of the fundamental it samples this excess noise, which then adds to the demodulated noise level. The quadrature

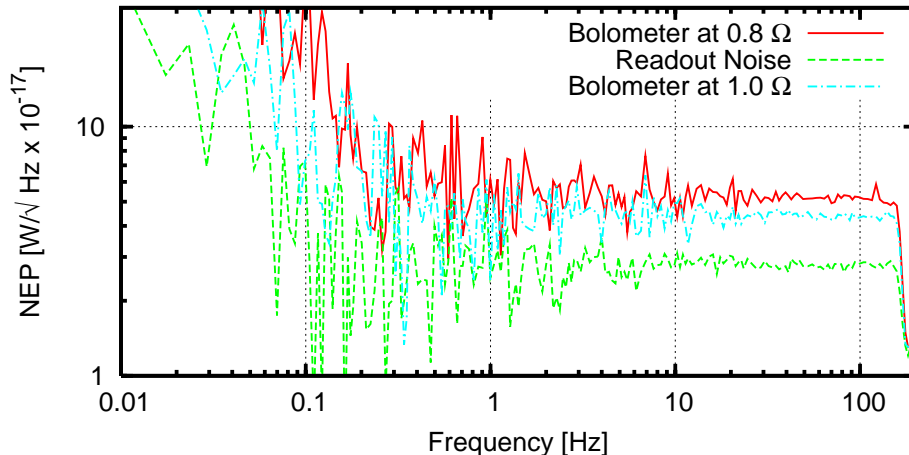


Figure 7. Demodulated noise of bolometer ‘9-03’ in NEP units biased into the transition (red, solid) and above the transition (blue, dot-dash). The green, dashed curve shows the readout noise level.

sum of the mixer’s response and the measured noise levels at odd harmonics of the demodulator frequency is  $3.0 \times 10^{-17} W/\sqrt{Hz}$  which matches the measured value. The excess demodulated noise can be addressed without hardware changes by filtering away harmonics with a low pass filter in firmware. The source of increased out of band noise above 1 MHz is currently unknown, but we have ruled out the bolometers as the source because the same out of band noise is observed in SQUIDS that are not connected to detectors.

Bolometer Johnson, SQUID and readout electronics NEP scale linearly with the voltage bias,  $V_b$ . In any astrophysical application, the radiative background loads the bolometer, and the voltage bias required to keep the TES in transition is smaller than the voltage bias needed for these dark measurements. If half the power required to keep these bolometers in the transition comes from radiative loading, the NEP from terms proportional to voltage bias summed in quadrature is  $1.0 \times 10^{-17} W/\sqrt{Hz}$  which is below the photon noise level at 150 GHz of  $2.5 \times 10^{-17} W/\sqrt{Hz}$ .

## 6. CONCLUSION

We have fabricated and measured a TES bolometer array as part of a program to produce low thermal conductance TES arrays for the EBEX balloon-borne experiment. Average thermal conductance measurements of three bolometers on the proto-type array are in good agreement with the 32 pW/K designed value. Noise measurements are 20% larger than expected. All measurements are taken with DfMUX readout electronics, which have been designed for low power consumption suitable for a balloon application.

Table 1. Noise expectation for dark bolometer ‘9-03.’

Noise source	Equation	NEP ( $10^{-17} W/\sqrt{Hz}$ )
Phonon <sup>17</sup>	$\sqrt{\gamma 4k_b T_c^2 G}$	2.3
Bolometer Johnson	$\sqrt{4k_b T_c / R} \cdot V_b$	1.9
SQUID	$2.5 pA_{rms} / \sqrt{Hz} \cdot V_b$	0.9
Readout electronics	$4.7 pA_{rms} / \sqrt{Hz} \cdot V_b$	1.7

Here  $\gamma = 0.498$ ,  $k_b$  is Boltzmann’s constant,  $T_c = 550$  mK,  $G = 63$  pW/K,  $R = 0.8 \Omega$  and  $V_b = 2.275 \mu V_{rms}$ .

With its design sensitivity and a 14 day flight, EBEX will either detect the signature of gravity waves from the epoch of inflation shortly after the big bang or will set a  $2\sigma$  upper bound of  $1.3 \times 10^{16}$  GeV on the energy scale at which inflation took place. The bolometer arrays and DfMUX readout boards will be tested in the balloon environment during the EBEX North American flight scheduled for Fall 2008.

## 6.1 Acknowledgments

EBEX is supported by NASA through grant numbers NNG05GO02H and NNX08AG40G. J. Hubmayr acknowledges support from the NASA Graduate Student Research Program (GSRP) and a Grant-In-Aid of Research (GIAR) from the National Academy of Sciences, administered by Sigma Xi, The Scientific Research Society. We thank K. Irwin and G. Hilton for providing SQUID arrays. M. Dobbs acknowledges the support of the Natural Sciences and Engineering Research Council of Canada (NSERC) and of the Canadian Institute for Advanced Research (CIFAR) through its Cosmology and Gravity Program.

## REFERENCES

- [1] Gildemeister, J. M., Lee, A. T., and Richards, P. L., “Monolithic arrays of absorber-coupled voltage-biased superconducting bolometer,” *Appl. Phys. Lett* **77**(24), 4040–4042 (2000).
- [2] Lee, S., Gildemeister, J. M., Holmes, W., Lee, A. T., and Richards, P. L., “Voltage-biased superconducting transition-edge bolometer with strong electrothermal feedback operated at 370 mK,” *Appl. Opt.* **37**, 3391–3397 (1998).
- [3] de Korte, P. A. J., Beyer, J., Deiker, S., Hilton, G. C., Irwin, K. D., MacIntosh, M., Nam, S. W., Reintsema, C. D., and Vale, L. R., “Time-division superconducting quantum interference device multiplexer for transition-edge sensors,” *Rev. Sci. Instrum.* **74**, 3087 (2003).
- [4] Lanting, T. M., Cho, H., Clarke, J., Dobbs, M., Lee, A. T., Richards, P. L., Smith, A. D., and Spieler, H. G., “A frequency-domain squid multiplexer for arrays of transition-edge superconducting sensors,” *IEEE Trans. Appl. Sup.* **13**(2), 626 (2003).
- [5] Dobbs, M. and N. Halverson *et al.*, “APEX-SZ first-light and instrument status,” *New Astronomy Reviews* **50**, 960–968 (2006).
- [6] J. Ruhl *et al.*, “The South Pole Telescope,” *Proc. SPIE Int. Soc. Opt. Eng.* **5543** (2004).
- [7] J. Fowler *et al.*, “The atacama cosmology telescope project,” *Proc. SPIE mm. & Sub-mm. Det. Ast. II* **5498**, 1–10 (2004).
- [8] P. Oxley *et al.*, “The EBEX experiment,” *Proc. SPIE Int. Soc. Opt. Eng.* **5543**, 320–331 (2004).
- [9] Dobbs, M., Bissonnette, E., and Spieler, H., “Digital frequency domain multiplexer for mm-wavelength telescopes,” *IEEE Transactions on Nuclear Science* **TNS-00230-2007.R2** (2008).
- [10] Irwin, K. D., Hilton, G. C., Wollman, D. A., and Martinis, J. M., “Thermal-response time of superconducting transition-edge microcalorimeters,” *J. Appl. Phys.* **83**(8), 3978–3985 (1998).
- [11] Holmes, W., Gildemeister, J. M., and Richards, P. L., “Measurements of thermal transport in low stress silicon nitride films,” *Appl. Phys. Lett* **72**, 2250–2252 (1998).
- [12] Lee, A. T., Richards, P. L., Nam, S. W., Cabrera, B., and Irwin, K. D., “A superconducting bolometer with strong electrothermal feedback,” *Appl. Phys. Lett* **69**(12), 1801–1803 (1996).
- [13] Chase, S., [*Two-stage sub-Kelvin  $^3\text{He}$  cooler*], Chase Research Cryogenics Ltd., 140 Manchester Road, Sheffield S10 5DL, England.
- [14] Panasonic, [*ECJ series*].
- [15] Huber, M. E., Neil, P. A., Benson, R. G., Burns, D. A., Corey, A. M., Flynn, C. S., Y.Kitaygorodskaya, Massihzadeh, O., Martinis, J. M., and Hilton, G. C., “DC SQUID series array amplifiers with 120 MHz bandwidth (corrected),” *IEEE Trans. Appl. Sup.* **11**(2), 4048–4053 (2001).
- [16] Spieler, H., “Frequency domain multiplexing for large scale bolometer arrays,” *Monterey Far-IR, Sub-mm and mm Detector Technology Workshop proceedings*, 243–249 (2002).
- [17] Mather, J., “Bolometer noise: nonequilibrium theory,” *Appl. Opt.* **21**(6), 1125–1129 (1982).